Construction and Building Materials 220 (2019) 110–118

Contents lists available at ScienceDirect

Construction and Building Materials

journal homepage: www.elsevier.com/locate/conbuildmat

Effect of nano-silica on hydration, microstructure of alkali-activated slag

Jinbang Wang, Peng Du, Zonghui Zhou *, Dongyu Xu, Ning Xie, Xin Cheng *

Shandong Provincial Key Laboratory of Preparation and Measurement of Building Materials, Engineering Center of Advanced Building Materials of Ministry of Education, University of Jinan, Jinan 250022, China

HIGHLIGHTS

- The microscopic morphology and hydration characteristics are optimized by adding nano-silica.
- The added nano-silica was consumed and it cannot act as filler due to its high activity.
- The hydration process was promoted due to nucleation effect and siliceous precursors supplied effect.
- The nano-silica action mechanisms on alkali-activated slag ware discussed.

ARTICLE INFO

Article history:
Received 26 December 2018
Received in revised form 12 March 2019
Accepted 25 May 2019
Available online 7 June 2019

Keywords:
Nano-silica
Hydration
Micro structural evolution
Alkali-activated slag

ABSTRACT

Hydration and micro-structure are important in the study of alkali-activated materials, especially used in building materials. To obtain information about hydration processes, we have investigated the hydration rate and micro-structural evolution. In this research, we evaluated the performances of nano-silica composite, which is produced by adding nano-silica into alkali activated slag. We also tested the impacts of nano-silica on hydration, micro-structure and porosity. Results of the experiments shows that the comprehensive strength is enhanced, the microscopic morphology and hydration characteristics are optimized. Also, hydration rate suggested that the impact of nano-silica on alkali activated slag early hydration is far greater than that of later hydration. Furthermore, the nano-silica action mechanisms on alkali-activated slag discussed in this paper mainly are that the nano-silica supplied siliceous precursor and served as nucleation seed and its accelerated early hydration effects.

1. Introduction

Alkali activated materials, which firstly invented and applied patent by Davidovits [1], were considered as alternative and supplementary materials to replace Ordinary Portland cement (OPC) with respect to reduce CO_2 emissions. This kind of materials was famous for its lower energy consumption than Portland cement and wider range of raw materials resources, such as blast furnace slag [2], waste glass [3], fly ash [4], rice husk ash [5], red mud, steel slag [6] and other industrial waste residue [7,8], which were difficult to use in large scale in cement production industry. The truth is, alkali-activated materials has an advantage over other building materials such as ceramics and Portland cement, for it providing many important performance advantages, for example, high early compressive strength [9], high freeze-thaw resistance [10], strong acid-base corrosion resistance [11], excellent impermeability [12] and outstanding fire resistance [1].

By now, it is generally believed that alkali-activated materials' hydration process has three stages [13]. The first stage is decomposition–coagulation reaction, which means that under strong alkaline condition, the alumino-silicate contained in raw materials depolymerized into ions. The second stage starts as the increase of precursor number and the reaction process accumulates. In the meantime, the third stage of condensation and crystallization happens, the hydrated calcium alumino-silicate gels and hydrated calcium silicate gels were produced in this stage [14]. Although the simulated hydration process had been discovered by research fellows [15,16], there are not many essays on how to characterize hydration mechanism of alkali-activated slag by the hydration exothermic rate.

Nowadays, nano technology plays a vital role in the field of cement and concrete industries [17]. The performances of certain cement based materials were affected by different nano materials [18]. Considering the fact that nano-silica were widely applied in cement-based materials and it might have similar effects in

* Corresponding authors.
E-mail addresses: mse_dup@ujn.edu.cn (P. Du), mse_zhouzh@ujn.edu.cn (Z. Zhou), mse_xudy@ujn.edu.cn (D. Xu), mse_xien@ujn.edu.cn (N. Xie), chengxin@ujn.edu.cn (X. Cheng).

https://doi.org/10.1016/j.conbuildmat.2019.05.158
0950-0618/

alkali-activated materials, modified alkali-activated materials with nano materials have received wide attention [19,20]. In the past ten years, it was reported that the performances of alkali-activated cementitious materials could be overwhelmingly enhanced to incorporate nano materials such as the early stage compressive strength [21] and sorptivity and acid resistance properties [22]. H. Assaedi et al. [23] pointed out that the compressive strength of geopolymer paste made from fly ash were increased by 23.39% when adding 2.0% nano-clay. The results showed that the geopolymer nano-composites adding 2.0 wt% nano-clay have better mechanical properties, for the nano-clay is acting as an activator to facilitate the geopolymeric reaction. A similar conclusion was drawn according to the research of H. M. Khater [20], he found the compressive strength cured for 28 days increased 17.06% when he prepared alkali-activated water cooled slag geopolymer nano-composites incorporating no more than 1.5 wt% nano-clay. L.Y. Yang et al. [24] enhanced the mechanical strength by 15.45% cured for 7 days and improved pore structure and decreased the shrinkage of alkali-activated slag nano-composites when he added 0.5 wt % nano-TiO_2.

The development of nano-silica production technology leads to the reduction of its production cost [25], utilization of nano-silica in cement and alkali activated cementing materials offered more advantages than other nano-materials [26]. Kang Gao [27] first reported that geopolymerization could be greatly accelerated attribute to the increase of speed and degree of polymerization and filling pores effect of nano-silica particles when he mixed 3.0% nano-silica, but the action mechanism of nano-silica particle was not clearly explained. H. Assaedi [28] did a research on the effect of nano-silica mixing methods on performances and micro-structural evolution of geopolymer paste prepared from fly ash. He came to conclusions that the micro-structure optimization and strength improvement were attributed to increasing of hydrated calcium alumino-silicate gels and hydrated calcium silicate gels. Partha Sarathi Deb [21] reached a similar conclusion and suggested that densification caused by nano-silica was another reason for microstructure optimization and strength growth. While Mohammed Ibrahim [29] believed that the application of nano-SiO_2 promotes the polymerization and formation efficiency of hydrated calcium aluminosilicate gels and hydrated sodium aluminosilicate gels. A nucleation was triggered and the induction period was reduced due to the generation of more geopolymeric gels in the early stage of 12–72 h when nano-silica added into fly ash-slag geoporlymer matrix according to research of T. Revathi et al. [30]. Fatemeh Shahrajabian and Kiachehr Behfarnia [31] did research on the frost resistance of slag concrete activating with water glass and incorporating nano materials. In the freezing and thawing cycles experiment, they found out that slag concrete modified with nano-silica and nano-clay have better strength values than nano-alumina. Abdulkadir Çevik et al. [32] found that mechanical strength after chemical corrosion were holonomy kept because of the generation of dense micro-structure with low porosity when 3.0 wt% nano silica (NS) was added to fly ash geopolymer concrete. However, K. Behfarnia [33] claimed that application of micro-silica has positive effect on microstructure while application of nano-silica possessed negative effects on microstructure due to the formation of tilleyite when incorporated micro-silica and nano-silica into alkali activated slag concrete.

Although there are essays about the performances and microstructural evolution [34] of alkali-activated composites modified with nano-silica. The effect of nano-silica on hydration mechanism and microstructural evolution in early stage is still not very clear, especial for question that how does nano-silica act on alkali-activated materials in a strong alkaline environment. Thus, this experiment aims to investigate the effects of nano-silica on early hydration process and micro-structural evolution and discuss its mechanism of action.

2. Materials and experiments

2.1. Materials

The main raw materials selected as alumino-silicate source were well ground steel slag powder and blast furnace slag powder, which provided by JIGANG GROUP co., ltd. And their fineness was determined as 389 m^2/kg and 421 m^2/kg using specific surface area meter. It was analyzed that chemical composing of raw materials and indicated in Table 1. A nano-meter silicon dioxide with average particle diameter 30 nm and purity of 99.95% were prepared by Beijing DC technology co. LTD. The specific surface area of nano-silica was tested as 200 m^2/g. An analytically pure chemical reagent sodium hydroxide flake was provided by DAMAO chemical reagent factory. Sodium hydroxide solution was selected as alkali-activator and it was beforehand prepared in order to cool to ambient temperature.

The particle diameter of waste powder was measured and presented in Fig. 1 and Fig. 2, respectively.

Nano-silica was dissolved in alcohol and dispersed by ultrasound and its particle diameter was tested and listed in Fig. 3. It was noted that the average size of nano-silica particle (Xav) was 92 nm and the median size of nano particle (X50) was 80 nm, which suggests that the size of dispersed nano-silica was larger than the average size purchased and the nano materials was prone to agglomeration [35].

2.2. Specimens preparation and test methods

Nano-silica in mass of 0.0%, 0.5%, 1.0%, 2.0% and 3.0% were used to replace the main raw materials such as waste powder. A ratio of 1:1 of slag-steel slag was adopted to improve utilization rate of steel slag. Analytical reagents sodium hydroxide was dissolved in distilled water until the solution cools to room temperature. The quality of sodium hydroxide accounted for 6.0% of the waste powder quality. The waste powder were weighed and mixed for 24 h in order to obtain well mixed materials according to proportion listed in Table 2. Considering the fact that the fluidity will be reduced after adding nano-materials, a slight high w/s ratio of 0.36 was used. The water used in the experiment was divided into two aspects, one aspect was for dissolving sodium hydroxide and another aspect was for dispersing nano-silica. An ultrasonic device (400 W, 40 kHz) was adopted according to related literatures, so as to disperse nano-silica particles into distilled water in order to avoid agglomeration [35,36]. The waste powder was first poured into mixing pot and then alkaline solution was slowly added and blended for 5mins, after that the dispersed nano-silica solution was intermixed to prepare the fresh paste. Then the fresh paste were quickly injected into the mold (20 × 20 × 20 mm) and moved to curing chamber (20 ± 2°C and 95 ± 5% R.H.).

Table 1
Chemical analysis of raw materials (wt%).

Component	Slag	Steel slag	Nano-silica
Cao	37.28	37.84	0.01
MgO	8.56	8.02	0.01
Fe_2O_3	0.65	24.78	0.01
Al_2O_3	16.34	6.16	0.01
SiO_2	32.48	14.65	99.66
Loss	1.63	1.42	0.01
Other	2.55	5.12	0.01

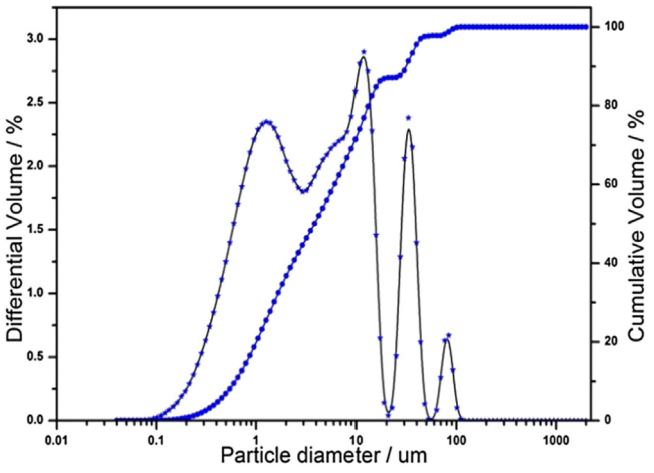

Fig. 1. The distribution of steel slag radius.

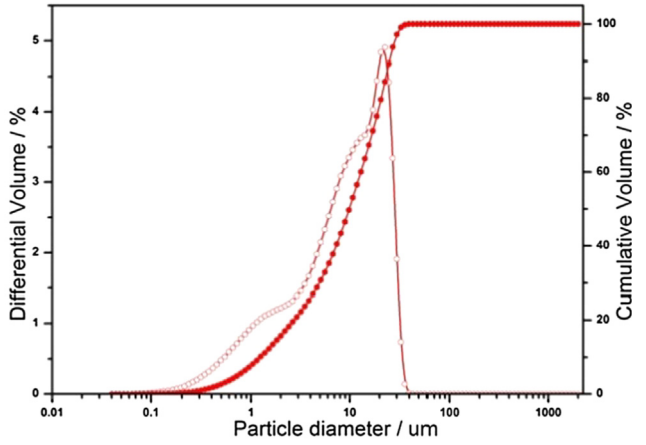

Fig. 2. The distribution of blast furnace slag radius.

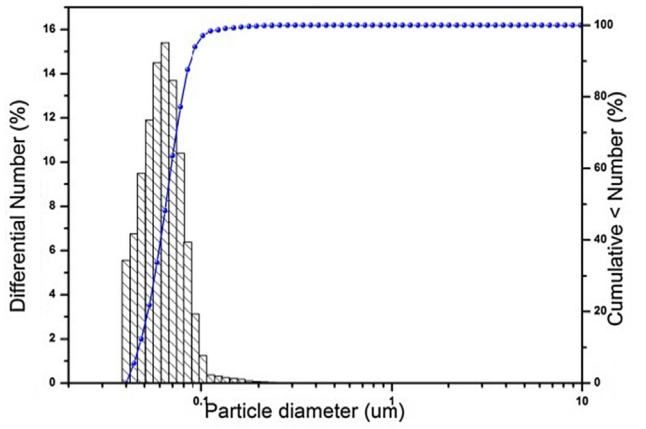

Fig. 3. The particle diameter of nano-silica.

The compressive strengths test were done according to ISO 679:2009 and specimens loading rate was set as 2400 N/s [37]. Pore size distribution of hardened paste was tested with Mercury Intrusion Pore method. The immersed specimens in an alcoholic solution were crushed and dried for 10 h at the temperature of 60 °C and tested under intrusion pressure of 0.53–59940.28 psia and extrusion pressure of 59940.28–20.21 psia. STA6000 thermal analyzer was used to conduct the TG tests at the temperature of 25–1000 °C and heating rate of 10 °C/min. TAM Air C80 isothermal calorimeter was selected to monitor and record the change of hydration heat and exothermic rate in early 72 h [38,39]. Water/binder ratio used in this experiment was 0.36 in order to stay the same with fresh paste. In order to find out whether or not there was unreacted nano-silica in the specimens that cured for 1d, hardened paste (including control samples and specimens with 2.0% and 3.0% nano-silica) of 0.9 g, which kept in alcohol and calcium hydroxide of 0.1 g were added to monitor hydration heat change in early 48 h. Water/binder ratio of 1.0 was adopted in rehydration heat experiment. A type of electron microscope branded Carl Zeiss Jena was adopted to observe the microstructural evolution of samples incorporating nano-silica. The specimens soaked in pure ethanol were smashed into pieces and dried for 2 h at 60 °C, and then sprayed with gold to keep good conductivity in the surface of specimens. XRD test was performed by Germany Brook D8 ADVANCE diffractometer at scanning speed of 4°s/step with voltage of 40 kV and current of 40 mA.

3. Results and discussion

3.1. Effect of nano-silica on hydration process

The heat of hydration test is in Fig. 4. According to relevant references [40,41], the hydration process of cement-based material and alkali-activated material characterized with exothermic rate curves were divided into five periods, namely initial hydration period, induction period, acceleration period, deceleration period and steady state period. Alkali-activated slag hydration process was similar to that of cement-based material as the curves presented in Fig. 4. Wetting heat and dissolving heat were the main causes for occurrence of the first hydration heat peak [41], which appears after around 500 s. Most of the decomposition and coagulation reaction happens in this period. As can be seen from Fig. 4a, exothermic rate was directly proportional to nano-silica dosage, and the peak value presented the same tendency, which showed the dissolution degree of slag and nano-silica increased and more precursors generated. Without nano-silica, specimens with 1.0%, 2.0% and 3.0% respectively take 465.3 s, 400.2 s, 319.2 s and 229.3 s to reach its peak value occurrence. The results showed that the time of peak occurrence was brought forward according to the increase of nano-silica dosage, which suggested that the dissolving process of precursors was accelerated. The reason might be that, unsaturated silicon bond in nano-silica combined the OH— to form ≡Si—OH, which could form hydrated calcium silicate gels by the chemical reaction between ≡Si—OH and $Ca(OH)_2$ [42]. The process can be sketched as follows [43].

$$\equiv Si - O - + H - OH ==\equiv Si - OH + OH - \ (\text{rapidly})$$

Table 2
The mixing ratio of paste inclusion of nano-silica.

Sequence number	Slag/(%)	Dosage of nano-silica/(%)	Liquid-solid ratio	C(NaOH)/mol/L	Slag/kg/m^3	Nano-silica/Kg/m^3	Water/kg/m^3
Control	100.0	0.0	0.36	4.17	1718.8	0.0	614.6
A1	99.5	0.5	0.36	4.17	1710.2	8.6	614.6
A2	99.0	1.0	0.36	4.17	1701.6	17.2	614.6
A3	98.0	2.0	0.36	4.17	1684.4	34.4	614.6
A4	97.0	3.0	0.36	4.17	1667.2	51.6	614.6

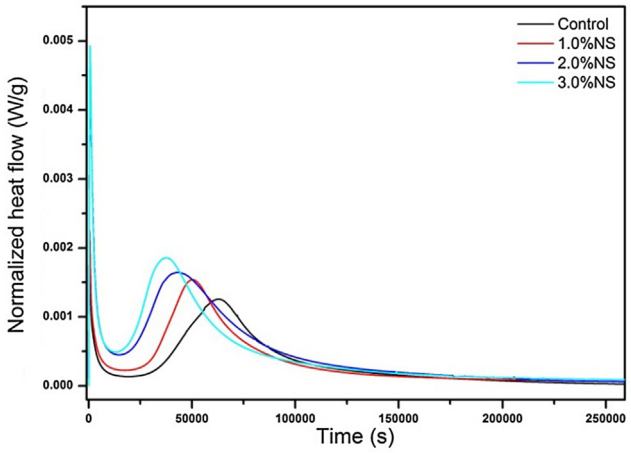

Fig. 4. Hydration exothermic rate curves of specimens.

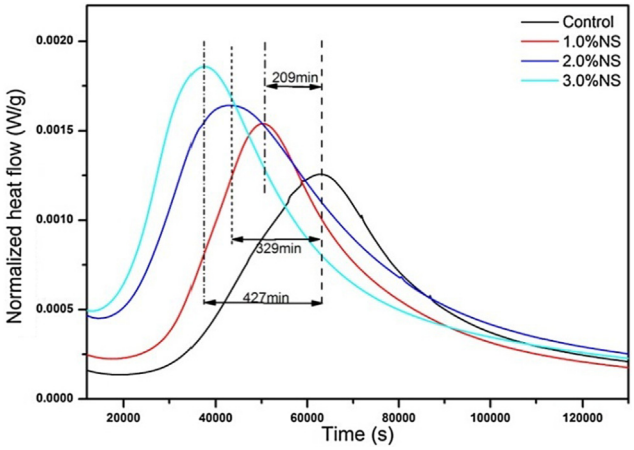

Fig. 4b. The enlarged partial view in Fig. 4.

$$\equiv Si - + OH - == \equiv Si - OH\,(\text{rapidly})$$

$$\equiv Si - OH + Ca(OH)_2 == C - S - H$$

So the added nano-silica served as nucleation sites, and it offers more initial point to generate hydrated calcium silicate gels, this assumption was consistent with the viewpoint by T. Revathi [30]. Another important result can be concluded from Fig. 4 and Fig. 4b is that the exothermic rate before first 100,000 s (27.78 h) was higher than that of later 100,000 s (27.78 h). So the impact of nano-silica on early stage hydration was far greater than that of later stage hydration. The information was consistent with compressive strength change laws, which means that strength growth rate of first day is much higher than that of the following 28 days.

The second sharp peak (showed in Fig. 4 and partial enlarged drawing in Fig. 4b) occurred at around 17 h, when covered acceleration period and deceleration period. It can be found that the exothermic rate value increased and the peak value appeared ahead of time with increasing of nano-silica. The results demonstrated that a massive precipitation of reaction products occur, which was in favour of geopolymeric gel formation. In comparison with the specimens without nano-silica, the second peak value separately appeared at 427 min, 329 min and 209 min in advance, which indicated that hydration process was greatly accelerated by incorporating nano-silica. The obtained results agreed with Phoongernkham [14] that have performed similar experiments. Also, the geopolymeric reaction was enhanced and the hydration products amount was increased. Homology mechanisms were also widely used in cement based nanocomposites. Sagoe-crentsil [44] believed incorporating of nano-silica evenly distributed in the matrix supplied more nucleation sites and promoted the polymerization of precursors.

The total hydration heat was tested and presented in Fig. 5. The results showed that the total heat of hydration increased as nano-silica dosage increase. The first reason is that the added nano-silica accelerated the hydration reaction. Its nucleation effect played a major role in the early stage. The second reason is that, according to relevant essay [29,32], nano-silica particles have large specific surface and high activity, which mean that parts of nano-silica was neutralized with alkali solution to release some heat. At 60,000 s, the total exothermic heat of specimens without 1.0%, 2.0% and 3.0% of nano-silica separately was 28.60, 45.28, 74.51 and 83.46 J/g. Compared to the control specimen, the total hydration heat of specimens incorporated 1.0 wt%, 2.0 wt% and 3.0 wt% nano-silica increased by 58.32%, 160.52% and 191.82%, respectively. However, the total heat increase rate decreased to 10.79%, 52.30% and 86.68% at the end of experiment (72 h). All the evidences made for a fact that impact of nano-silica on total hydration heat mainly lies in early hydration.

3.2. Effect of nano-silica on compressive strength

The changes that compressive strength brings to specimens without nano-silica and with 0.5%, 1.0%, 2.0%, 3.0% of nano-silica

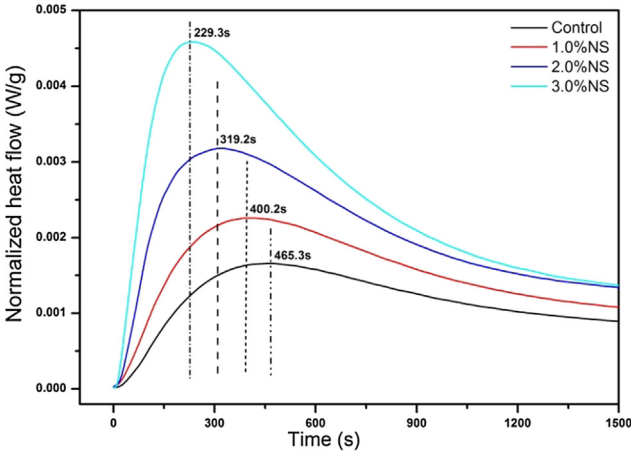

Fig. 4a. The enlarged partial view in Fig. 4.

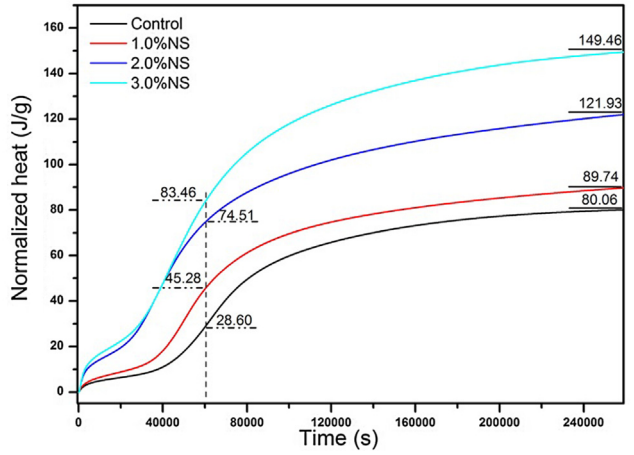

Fig. 5. Total hydration heat release curves of samples.

were listed in Fig. 6. It can be found out that compressive strength presents similar growth orderliness. Namely, with the increase of nano-silica, the strength value first increased rapidly and then decreased slowly and the maximize occured when the dosage of nano-silica was 2.0 wt%. It is noticed that strength value of control samples (0.0% nano-silica) cured 1 day increased from 21.2 MPa to 34.8 MPa (2.0 wt% nano-silica) and that of the control samples cured 3 days increased from 29.7 MPa to 41.2 MPa (2.0 wt% nano-silica) and 28 days strength value from 48.8 MPa (0.0% nano-silica) increased to 54.7 MPa (2.0 wt% nano-silica). And the strength growth rate cured for 1d, 3d and 28d could be calculated according to the data above. Compared to the control sample (without nano-silica), the strength growth rate cured for 1d, 3d and 28d were respectively 64.15%, 38.72% and 18.24%. The results revealed that early strength growth of alkali activated slag promoting by nano-silica were much better than later stage strength growth.

Based on three major roles of nano-silica, there are three reasons. The first and the most important reason is that the addition of high activity nano-silica supplied siliceous raw materials, which means that the parts of nano-silica was consumed by alkali solution to produce more silicon monomer (precursors) and promoted the geological polymerization. It was one reason why the hydration reaction rate was accelerated. The second reason is that more hydration products were generated. For instance, hydrated calcium silicate gels, which filled the pores, decreased the porosity, increased the compactness and improved the strength [45]. The reaction of nano-silica and alkali solution worked in early stage. It also explains that the growth rate of compressive strength in early stage was higher than that of late stage. Secondly, nano-silica also acts as nucleation seed, which provided more nucleation sites and facilitated the generation of hydrated calcium aluminosilicate gels hydrated calcium silicate gels and reduce the induction period in early period of 12–72 h [30], this was another main reason why hydration rate was accelerated and why nano-silica influenced emphatically on early strength. The assumption showed no difference with Khater [20] and Riahi [46], and this assumption consistent with experimental results that the strength did not rise continuously as increasing of nano-silica dosage but decreased when a threshold (2.0 wt% nano-silica) surpassed. Because that the number of nano-silica acted as nucleation seed was limited, superabundant nano-silica were not increase the number of effective nucleation seed, but easy to agglomeration and take water in the solution and hinder the geological polymerization [47]. What is more, more pores and defects were brought in specimens and decreased the compressive strength according to Gomez-Zamorano L.Y. [48].

Thirdly, added nano-silica may act as filler, which was based on the fact that the added nano-silica did not completely react with the alkali solution. In order to find out if there was unreacted nano-silica in the specimens that cured for 1d, rehydration heat experiments were conduct and the results were listed in Fig. 7. As noted in Fig. 7 that, there was one peak, which stood for initial dissolution heat. If there was unreacted nano-silica in the specimens after curing for 1d, there must be another peak heat of reaction from unreacted nano-silica and calcium hydroxide added in the experiment in addition to the initial heat of dissolution. Thus, it was easy to see that the added nano-silica cannot act as filler and all the nano-silica added in specimens was consumed or reacted in the strong alkali solution after the specimens cured for 1d.

3.3. Effect of nano-silica on micro-structures

3.3.1. Effect of nano-silica on pore structure

Mercury intrusion pore experiments (MIP) were done to obtain more messages on hydration mechanism and obtained results were showed in Fig. 8 and Fig. 9. The control specimen (with 0.0% nano-silica) and 1.0%, 2.0% and 3.0% were selected to analyze the pores size distribution. It is considered that pores of different sizes have different effects on cement based materials, three classes of pore size were divided to macropores (>50 nm), mesopores (2–50 nm) and micropores (<2nm) [49]. As seen in Fig. 8, specimens are highest in mesopores and lowest in micropores and macropores, the amount of macropores (50 nm-200 nm) decreased with dosage of nano-silica and the amount of macropores (larger than 200 nm) for four specimens were nearly the same. However, as for the mesopores, the number of mesopores in turn decreases from the control specimens to specimens adding 1.0 wt%, 2.0 wt% and 3.0 wt%. With regard to micropores (0–2 nm), the content of micropores in turn decreases from specimens incorporating 3.0 wt%, 2.0 wt% and 1.0 wt% to the control sample. All the results revealed content of macropores and mesopores decreased significantly based on generation of more gels and itself filling effect and the induction nucleation effect of nano-materials [30]. Therefore, the pores size distribution was effectively improved and the micro-structure was fully optimized. Fig. 9 showed the total porosity of specimens with 0.0%, 1.0%, 2.0% and 3.0% nano-silica. It shows that total porosity decreases along with the increasing of nano-silica dosage, which suggests that hydration reaction was accelerated and more hydration products were produced and compactness was increased [29,50].

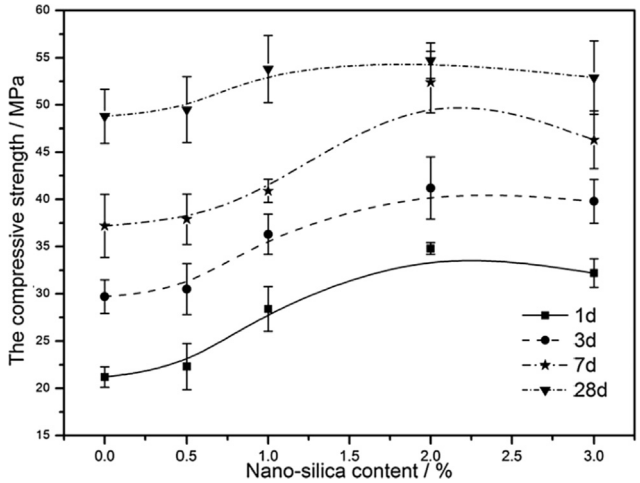

Fig. 6. Strength development of specimens with nano-silica.

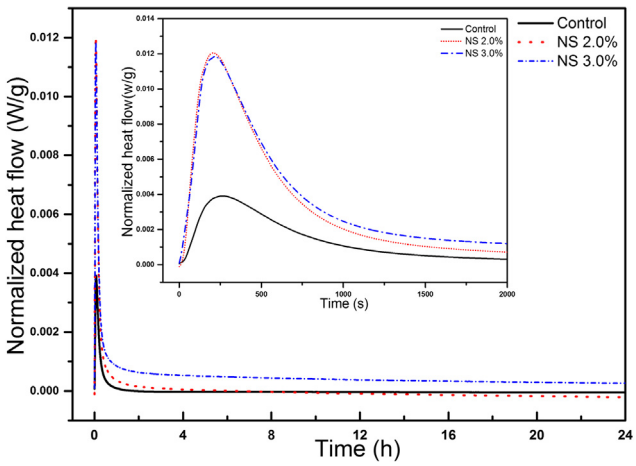

Fig. 7. Rehydration exothermic rate curves of specimens.

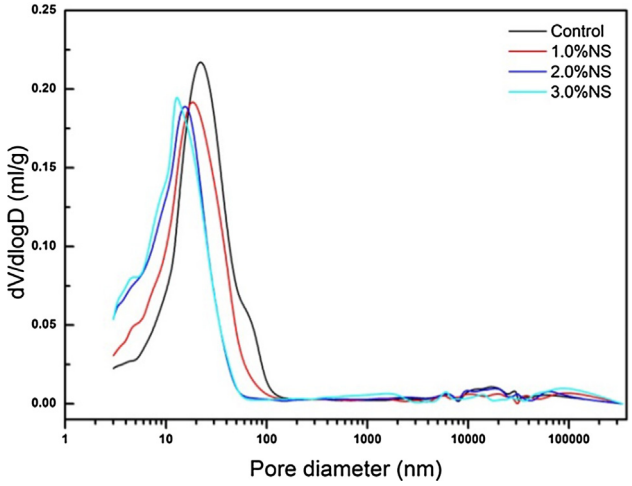

Fig. 8. Pore size distribution of specimens.

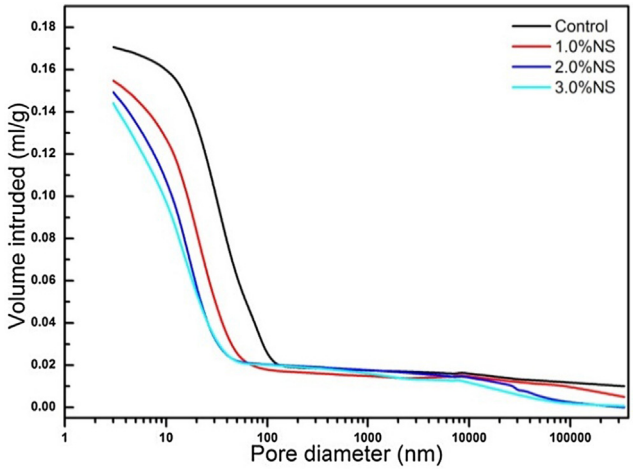

Fig. 9. Accumulative pore volume of specimens.

3.3.2. TG characterization

The thermo gravimetric test was performed and obtained results were illustrated in Fig. 10. Fig. 10 shows that, as the temperature increased, the specimen adding 3.0 wt% nano-silica gained more weightlessness than specimen incorporating 2.0 wt %, 1.0 wt% and the control specimen (0.0% nano-silica), which reflected that more hydrates were formed and the evidence derived from more weightlessness at the same temperature. It can be observed in the 1st derived curves that the weight loss between 25 and 100 was due to dehydration reaction of free water [51]. The degradation that happened at temperature of 100-300 was caused by dehydration reaction of combined water in hydrated calcium silicate gels. The results revealed that more hydrated calcium silicate gels were generated with increase of nano-silica dosage, which consistent with the compressive strength results. The formation of more hydration products will inevitably lead to a denser microstructure, which is a major reason for the increase in compressive strength [45]. When the temperature went up to 360-400 , a small weight loss occurred, possibly because $Ca(OH)_2$ decomposed into calcium oxide and combined water, while $Ca(OH)_2$ might formed from lower solubility and the reaction of Ca^{2+} ions and OH^- ions. Another small weight loss can be noted at 700 °C, which might be caused by the decomposition of $CaCO_3$ produced by carbonization of $Ca(OH)_2$.

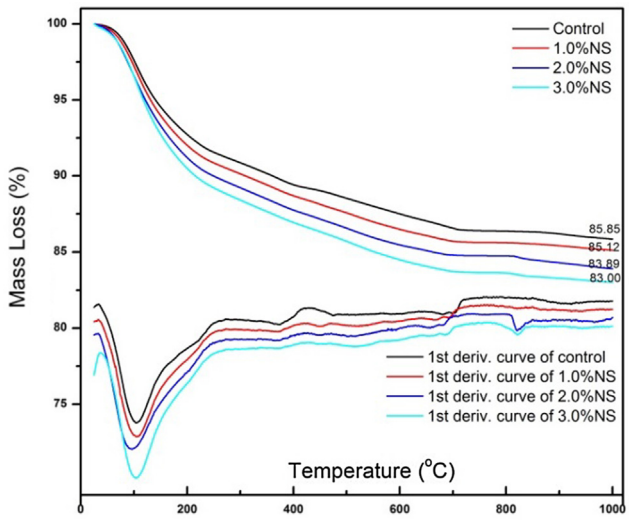

Fig. 10. TG curves of specimens inclusion of nano-silica.

3.3.3. SEM characterization

The specimens SEM pictures with nano-silica 0.0 wt%, 2.0 wt% and 3.0 wt% nano-silica cured for 1 day, 3 days and 28 days were respectively listed in Fig. 11(a), (b), (c), Fig. 11(d), (e), (f) and Fig. 11(g), (h), (i). Compared with Fig. 11(a), (b), 11(d), (e) and 11 (g), (h), it was not difficult to find out that the more gelatinous hydration products was generated, the denser micro-structures were, and the nano-silica amount increases, too. From Fig. 11(a), a porous microstructure could be clearly discovered, and no crystal products with hexagonal plate shape that probably be calcium hydroxide [52] were found in the porous structure. Usually, the calcium hydroxides were generated from the reaction of OH^- and Ca^{2+} and deposited in cavity where supplied enough crystal growth space in early hydration stage [53]. The assumption was also verified by thermogravimetric results illustrated in Fig. 10. Nevertheless, none of crystal products calcium hydroxide were noted in Fig. 11(d) and (g), the reason might be that the newly formed calcium hydroxide reacted with highly active nano-silica to generate hydrated calcium silicate gels, so this reaction mechanism was similar to volcanic ash effect of nano-silica [42] in cement-based materials. Less cracks and more gelatinous hydration production and dense micro-structure were produced according to the comparison of Fig. 11(c), (f), and (i), which may be the main reason for its compressive strength growth incorporating nano-silica. Another thing to note was that no unreacted nano-silica particles were found in Fig. 11(d) and (g), which also indicated that nano-silica was difficult to be stable in strong alkali environment for 1 day. The result obtained was consistent with rehydration exothermic rate curves, which showed in Fig. 7.

3.3.4. XRD characterization

XRD patterns of specimens cured for 1 day and 28 days were presented in Fig. 12 and Fig. 13. Figs. 12 and 13 indicates that the main mineral constituent were hydrated calcium alumino-silicate gels and hydrated calcium silicate gels, tetracalcium alumino-ferrite and RO phase [54]. Generally speaking, RO phase, tetracalcium alumino-ferrite mineral were not easy to be depolymerized and participate in the reaction, which would exist in the final products. An obvious variation tendency can be found in Fig. 12 that, the peak intensity between 28.3 and 34.4°2θ increased greatly with the accumulation of nano-silica dosage, which suggested that the amount of main products that hydrated calcium alumino-silicate gels and hydrated calcium silicate gels increased incorporating nano-silica and the evidence also reflected from

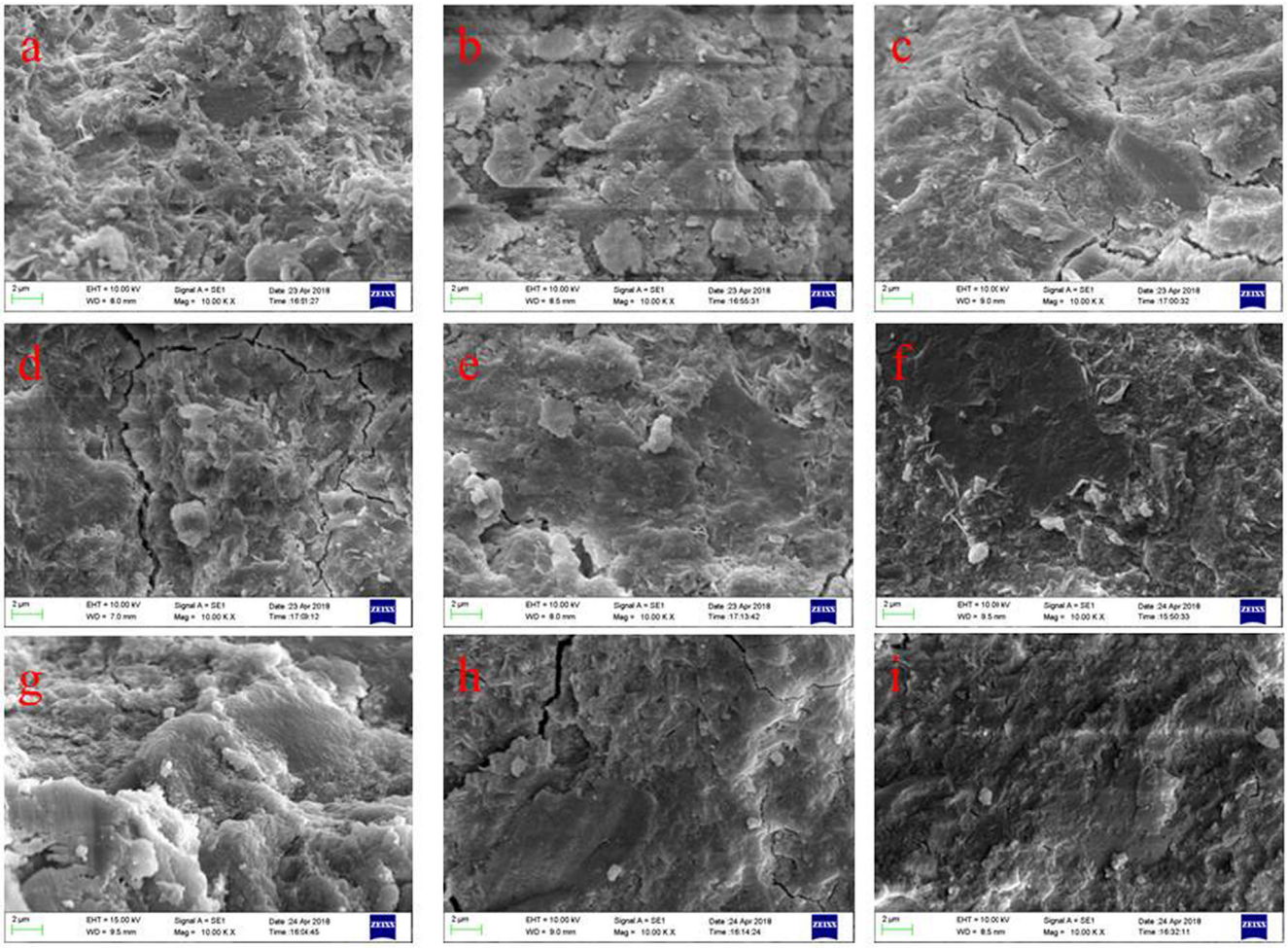

Fig. 11. SEM pictures of specimens cured for different days.

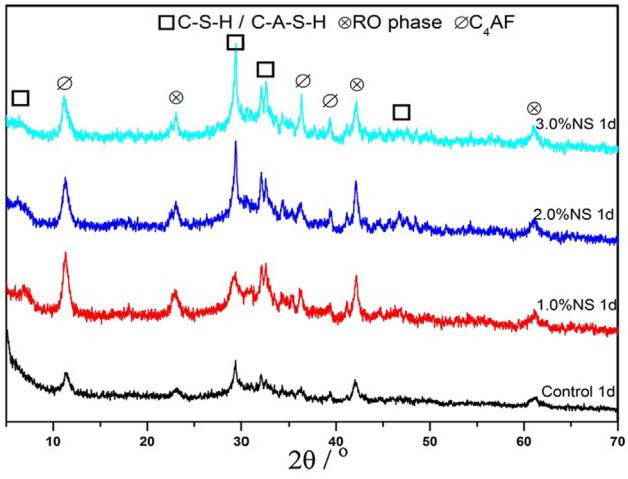

Fig. 12. X-ray diffraction patterns of samples cured for 1 day.

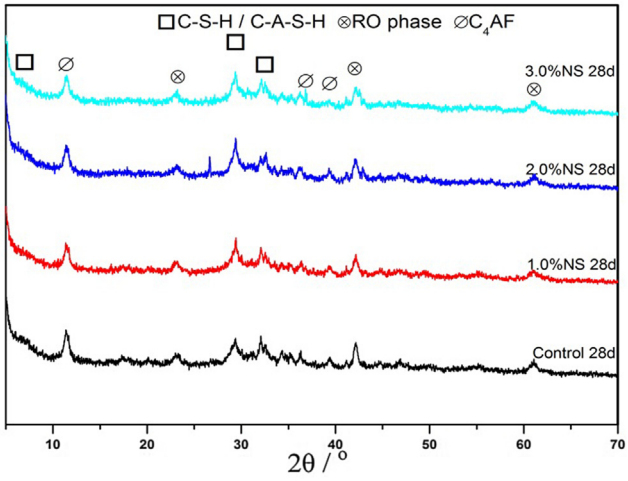

Fig. 13. X-ray diffraction patterns of samples cured for 28 days.

the SEM picture in Fig. 10. Although the peak intensity increased as can be noted in Fig. 13, it was not as significant as that in Fig. 12. Therefore, it can be verified that the hydration process were improved especially in early stage, which brought up the fine result that the formation of more gel products and the improvement of denser micro-structures.

4. Concluding remarks

1. The compressive strengths at early stage and late stage increased by 64.15% and 18.24%, the strength at early stage were affected more than late stage when adding nano-silica, owning to the high activity of nano-silica and it supplied siliceous precursors.

2. The hydration process was promoted and the nano-silica mainly affected hydration process at early stage rather than that of later stage. The added nano-silica cannot act as filler due to its high activity, not to mention that it is easily consumed in the strong alkali solution in the early stage.
3. The pore size distribution of hardened paste and its microstructures were effectively improved due to more hydration products generated, the mesopores increased, micropores and total porosity decreased when adding nano-silica into alkali-activated materials.

Acknowledgements

This research was funded from National Key Research and Development Program of China (2017YFB0309905), National Natural Science Foundation of China (No. 51702121), National Natural Science Foundation of China (No. 51872120), National High-tech Research and Development Program of China (863program) (2015AA034701), 111 Project of International Corporation on Advanced Cement-based Materials (No. D17001), Shandong Province Science and Technology Major Project (new industry) (2015ZDXX0702B01).

Declaration of Competing Interest

The authors declare no conflict of interest.

References

[1] J. Davidovits, 30 Years of Successes and Failures in Geopolymer Applications. Market Trends and Potential Breakthroughs. Geopolymer 2002 Conference. 2002, 1–16.
[2] T. Bakharev, J.G. Sanjayan, Y.B. Cheng, Resistance of alkali-activated slag concrete to acid attack, Cem. Concr. Res. 33 (10) (2003) 1607–1611.
[3] H.K. Tchakouté, C.H. Rüscher, S. Kong, E. Kamseu, C. Leonelli, Geopolymer binders from metakaolin using sodium waterglass from waste glass and rice husk ash as alternative activators: a comparative study, Constr. Build. Mater. 114 (2016) 276–289.
[4] C. Tennakoon, K. Sagoe-Crentsil, R. San Nicolas, J.G. Sanjayan, Characteristics of Australian brown coal fly ash blended geopolymers, Constr. Build. Mater. 101 (2015) 396–409.
[5] H.K. Tchakouté, C.H. Rüscher, S. Kong, N. Ranjbar, Synthesis of sodium waterglass from white rice husk ash as an activator to produce metakaolin-based geopolymer cements, J. Build. Eng. 6 (2016) 252–261.
[6] M.S.H. Khan, A. Castel, A. Akbarnezhad, S.J. Foster, M. Smith, Utilisation of steel furnace slag coarse aggregate in a low calcium fly ash geopolymer concrete, Cem. Concr. Res. 89 (2016) 220–229.
[7] L.N. Tchadjié, J.N.Y. Djobo, N. Ranjbar, H.K. Tchakouté, B.B.D. Kenne, A. Elimbi, et al., Potential of using granite waste as raw material for geopolymer synthesis, Ceram. Int. 42 (2) (2016) 3046–3055.
[8] A. Vásquez, V. Cárdenas, R.A. Robayo, R.M. de Gutiérrez, Geopolymer based on concrete demolition waste, Adv. Powder Technol. 27 (4) (2016) 1173–1179.
[9] J.L. Provis, Geopolymers and other alkali activated materials: why, how, and what?, Mater Struct. 47 (1–2) (2013) 11–25.
[10] Y. Fu, L. Cai, W. Yonggen, Freeze–thaw cycle test and damage mechanics models of alkali-activated slag concrete, Constr. Build. Mater. 25 (7) (2011) 3144–3148.
[11] C. Shi, Corrosion resistance of alkali-activated slag cement, Adv. Cem. Res. 15 (2003) 77–81.
[12] H. El-Didamony, A.A. Amer, H. Abd Ela-ziz, Properties and durability of alkali-activated slag pastes immersed in sea water, Ceram. Int. 38 (5) (2012) 3773–3780.
[13] A. Fernández-Jiménez, A. Palomo, Characterisation of fly ashes. Potential reactivity as alkaline cements, Fuel 82 (18) (2003) 2259–2265.
[14] T. Phoo-ngernkham, P. Chindaprasirt, V. Sata, S. Hanjitsuwan, S. Hatanaka, The effect of adding nano-SiO_2 and nano-Al_2O_3 on properties of high calcium fly ash geopolymer cured at ambient temperature, Mater. Des. 55 (2014) 58–65.
[15] Z. Zhang, H. Wang, J.L. Provis, F. Bullen, A. Reid, Y. Zhu, Quantitative kinetic and structural analysis of geopolymers. Part 1. The activation of metakaolin with sodium hydroxide, Thermochim. Acta 539 (2012) 23–33.
[16] Z. Zhang, J.L. Provis, H. Wang, F. Bullen, A. Reid, Quantitative kinetic and structural analysis of geopolymers. Part 2. Thermodynamics of sodium silicate activation of metakaolin, Thermochim. Acta 565 (2013) 163–171.
[17] H. Du, S. Du, X. Liu, Durability performances of concrete with nano-silica, Constr. Build. Mater. 73 (2014) 705–712.
[18] L. Senff, D. Hotza, S. Lucas, V.M. Ferreira, J.A. Labrincha, Effect of nano-SiO2 and nano-TiO2 addition on the rheological behavior and the hardened properties of cement mortars, Mater. Sci. Eng., A 532 (2012) 354–361.
[19] K. Gao, K.-L. Lin, D. Wang, C.-L. Hwang, B.L. Anh Tuan, H.-S. Shiu, et al., Effect of nano-SiO2 on the alkali-activated characteristics of metakaolin-based geopolymers, Constr. Build. Mater. 48 (2013) 441–447.
[20] H.M. Khater BAE-S, M. Fanny, M. Ezzat, M. Lottfy, A.M. El Nagar, Effect of nano-clay on alkali activated water-cooled slag geopolymer, Br. J. Appl. Sci. Technol. 3 (2) (2013) 764–776.
[21] P.S. Deb, P.K. Sarker, S. Barbhuiya, Effects of nano-silica on the strength development of geopolymer cured at room temperature, Constr. Build. Mater. 101 (2015) 675–683.
[22] P.S. Deb, P.K. Sarker, S. Barbhuiya, Sorptivity and acid resistance of ambient-cured geopolymer mortars containing nano-silica, Cem. Concr. Compos. 72 (2016) 235–245.
[23] H. Assaedi, F.U.A. Shaikh, I.M. Low, Effect of nano-clay on mechanical and thermal properties of geopolymer, J. Asian Ceram. Soc. 4 (1) (2016) 19–28.
[24] L.Y. Yang, Z.J. Jia, Y.M. Zhang, J.G. Dai, Effects of nano-TiO2 on strength, shrinkage and microstructure of alkali activated slag pastes, Cem. Concr. Compos. 57 (2015) 1–7.
[25] L.P. Singh, D. Ali, U. Sharma, Studies on optimization of silica nanoparticles dosage in cementitious system, Cem. Concr. Compos. 70 (2016) 60–68.
[26] A. Nazari, J.G. Sanjayan, Hybrid effects of alumina and silica nanoparticles on water absorption of geopolymers: application of Taguchi approach, Measurement 60 (2015) 240–246.
[27] K. Gao, K.-L. Lin, D. Wang, C.-L. Hwang, H.-S. Shiu, Y.-M. Chang, et al., Effects SiO2/Na2O molar ratio on mechanical properties and the microstructure of nano-SiO2 metakaolin-based geopolymers, Constr. Build. Mater. 53 (2014) 503–510.
[28] H. Assaedi, F.U.A. Shaikh, I.M. Low, Influence of mixing methods of nano silica on the microstructural and mechanical properties of flax fabric reinforced geopolymer composites, Constr. Build. Mater. 123 (2016) 541–552.
[29] M. Ibrahim, M.A.M. Johari, M. Maslehuddin, M.K. Rahman, Influence of nano-SiO2 on the strength and microstructure of natural pozzolan based alkali activated concrete, Constr. Build. Mater. 173 (2018) 573–585.
[30] T. Revathi, R. Jeyalakshmi, N.P. Rajamane, Study on the role of n-SiO2 incorporation in thermo-mechanical and microstructural properties of ambient cured FA-GGBS geopolymer matrix, Appl. Surface Sci. 449 (2018) 322–331.
[31] F. Shahrajabian, K. Behfarnia, The effects of nano particles on freeze and thaw resistance of alkali-activated slag concrete, Constr. Build. Mater. 176 (2018) 172–178.
[32] A. Çevik, R. Alzeebaree, G. Humur, A. Niş, M.E. Gülşan, Effect of nano-silica on the chemical durability and mechanical performance of fly ash based geopolymer concrete, Ceram. Int. 44 (11) (2018) 12253–12264.
[33] K. Behfarnia, M. Rostami, Effects of micro and nanoparticles of SiO2 on the permeability of alkali activated slag concrete, Constr. Build. Mater. 131 (2017) 205–213.
[34] D. Adak, M. Sarkar, S. Mandal, Effect of nano-silica on strength and durability of fly ash based geopolymer mortar, Constr. Build. Mater. 70 (2014) 453–459.
[35] D. Kong, X. Du, S. Wei, H. Zhang, Y. Yang, S.P. Shah, Influence of nano-silica agglomeration on microstructure and properties of the hardened cement-based materials, Constr. Build. Mater. 37 (2012) 707–715.
[36] P. Hou, K. Wang, J. Qian, S. Kawashima, D. Kong, S.P. Shah, Effects of colloidal nanoSiO2 on fly ash hydration, Cem. Concr. Compos. 34 (10) (2012) 1095–1103.
[37] ISO 679: Cement-Test methods-Determination of strength. International Standards Organization. 2009.
[38] Y. Huang, C. Xu, H. Li, Z. Jiang, Z. Gong, X. Yang, et al., Utilization of the black tea powder as multifunctional admixture for the hemihydrate gypsum, J. Cleaner Prod. 210 (2019) 231–237.
[39] X. Yang, J. Liu, H. Li, L. Xu, Q. Ren, L. Li, Effect of triethanolamine hydrochloride on the performance of cement paste, Constr. Build. Mater. 200 (2019) 218–225.
[40] Q.J.Y. Haijin Zhao, Jiang Xiong Wei, Jian Xin Li, Effect on structure and early hydration activity of steel slag modified by adjusting materials and temperature, Adv. Mater. Res. 24 (12) (2011) 163–168.
[41] A.P.F. Fernandez-Jimenez, A. Arteaga, Determination of kinetic equations of alkaline activation of blast furnace sl. determination of kinetic equations of alkaline activation of blast furnace slag by means of calorimetric data. J. Thermal Anal. Calorimetry, 1998, 52(3), 945–955.
[42] Z. Xu, Z. Zhou, P. Du, X. Cheng, Effects of nano-limestone on hydration properties of tricalcium silicate, J. Therm. Anal. Calorim. 129 (1) (2017) 75–83.
[43] Y. Qing, Z. Zenan, K. Deyu, C. Rongshen, Influence of nano-SiO2 addition on properties of hardened cement paste as compared with silica fume, Constr. Build. Mater. 21 (3) (2007) 539–545.
[44] L. Weng, K. Sagoe-Crentsil, Dissolution processes, hydrolysis and condensation reactions during geopolymer synthesis: Part I—Low Si/Al ratio systems, J. Mater. Sci. 42 (9) (2007) 2997–3006.
[45] P.D. Silva, K. Sagoe-Crenstil, V. Sirivivatnanon, Kinetics of geopolymerization: Role of Al2O3 and SiO2, Cem. Concr. Res. 37 (4) (2007) 512–518.
[46] S. Riahi, A. Nazari, The effects of nanoparticles on early age compressive strength of ash-based geopolymers, Ceram. Int. 38 (6) (2012) 4467–4476.
[47] Z. Zuhua, Y. Xiao, Z. Huajun, C. Yue, Role of water in the synthesis of calcined kaolin-based geopolymer, Appl. Clay Sci. 43 (2) (2009) 218–223.

[48] L.Y. Gomez-Zamorano, E. Vega-Cordero, L. Struble, Composite geopolymers of metakaolin and geothermal nanosilica waste, Constr. Build. Mater. 115 (2016) 269–276.
[49] K.S. Sing, Reporting physisorption data for gassolid systems with special reference to the determination of surface area and porosity, Pure Appl. Chem. 57 (4) (1984) 603–619.
[50] Z. Zhang, J.L. Provis, A. Reid, H. Wang, Fly ash-based geopolymers: the relationship between composition, pore structure and efflorescence, Cem. Concr. Res. 64 (2014) 30–41.
[51] C.A. Rosas-Casarez, S.P. Arredondo-Rea, J.M. Gómez-Soberón, J.L. Alamaral-Sánchez, R. Corral-Higuera, M.J. Chinchillas-Chinchillas, et al., Experimental study of XRD, FTIR and TGA techniques in geopolymeric materials, Int. J. Hous. Sci. Appl. 4 (4) (2014) 221–227.
[52] P.J.B.L. Schilling, A. Roy, H.C. Eaton, 29Si and 27Al MAS-NMR of NaOH-activated blast-furnace slag, J. Am. Ceram. Soc. 77 (9) (1994) 2363–2368.
[53] P.J.R.A. Schilling, H. Eaton, P.G. Malone, N.W. Brabston, Microstructure, strength, and reaction products of ground granulated blast-furnace slag activated by highly concentrated NaOH solution, J. Mater. Res. 9 (01) (1994) 188–197.
[54] B. Pang, Z. Zhou, H. Xu, Utilization of carbonated and granulated steel slag aggregate in concrete, Constr. Build. Mater. 84 (2015) 454–467.